JOURNAL OF GUIDANCE, CONTROL, AND DYNAMICS
Vol. 29, No. 5, September–October 2006

Periodic Relative Motion Near a Keplerian Elliptic Orbit with Nonlinear Differential Gravity

Prasenjit Sengupta,* Rajnish Sharma,† and Srinivas R. Vadali‡
Texas A&M University, College Station, Texas 77843-3141

DOI: 10.2514/1.18344

This paper presents a perturbation approach for determining relative motion initial conditions for periodic motion in the vicinity of a Keplerian elliptic orbit of arbitrary eccentricity, as well as an analytical solution for the relative orbit that accounts for quadratic nonlinearities in the differential gravitational acceleration. The analytical solution is obtained in the phase space of the rotating coordinate system, centered at the reference satellite, and is developed in terms of a small parameter relating relative orbit size, and semimajor axis and eccentricity of the reference orbit. The results derived are applicable for arbitrary epoch of the reference satellite. Relative orbits generated using the methodology of this paper remain bounded over much longer periods in comparison to the results obtained using other approximations found in the literature, because the semimajor axes of the satellites are shown to be matched to the second order in the small parameter. The derived expressions thus serve as excellent guesses for initiating a numerical procedure for matching the semimajor axes of the two satellites. Several examples support the claims in this paper.

Introduction

FORMATION flying of spacecraft is an area of recent interest wherein the study of the dynamics and control of relative motion is a key element. The applications of such formations are varied, including terrestrial observation, communication, and stellar interferometry. Most often, periodic or bounded relative orbits are desired for long-term formation maintenance, during the periods when maneuvers are not called for. A set of benchmark problems for spacecraft formation flying missions has been proposed by Carpenter et al. [1], that include reference low Earth orbit (LEO) and highly elliptical orbit (HEO) missions. An example of the latter is the Magnetosphere Multiscale mission (MMS) [2], where the apogee and perigee are of the order of $12–30R_e$ and $1.2R_e$, respectively, (with R_e denoting the radius of the Earth), yielding eccentricities of the order of 0.8 and higher. The theoretical development in this paper primarily concentrates on cases where the reference orbit has high eccentricity, while treating LEO missions as a special case.

The most common model describing relative motion near a Keplerian orbit is given by the Hill–Clohessy–Wiltshire (HCW) equations [3]. This model assumes a circular reference orbit and linearized differential gravity model, based on the two-body problem. Conditions for bounded motion, designated as HCW initial conditions, can be easily derived for this model and they have found wide applicability for formation flight. Though the relative motion between two spacecraft in Keplerian orbits is always bounded, for the purpose of formation flight, the term bounded as used in this paper refers to 1:1 resonance where the periods of all spacecraft are the same. The applicability of the HCW conditions is limited when any of the underlying assumptions are violated, viz. eccentric reference orbit, nonlinear differential gravity, aspherical Earth, and other perturbations. Because these factors accurately represent the realities of any mission, modifications to the model must be made to account for, and negate if possible, these effects. Previous work, limiting attention only to the two-body problem, may be categorized into those that deal with 1) nonlinear differential gravity, 2) noncircular reference orbit, and 3) the combination of nonlinearity and noncircular orbits. References [4–7] treated second-order nonlinearities as perturbations to the HCW equations and found approximate solutions to the system. Richardson and Mitchell [7] also included the solution to the third-order perturbed equation, with periodicity conditions enforced on the linear equation. The eccentricity problem has been treated by using either time or true anomaly as the independent variable. The linear problem for eccentric reference orbits was introduced by Tschauner and Hempel [8]. De Vries [9] obtained analytical expressions for relative motion using the Tschauner–Hempel (TH) equations, accurate to first order in eccentricity. Kolemen and Kasdin [10] also obtained a closed-form solution to periodic relative motion by treating eccentricity as a perturbation to a Hamiltonian formulation of the linearized HCW equations. The TH equations admit solutions in the form of special integrals, which have been derived in [11–13]. These solutions have been used to obtain state transition matrices for relative motion near an orbit of arbitrary eccentricity [14,15] using true anomaly as the independent variable, assuming a linearized differential gravity field. State transition matrices for relative motion using time as the independent variable have also been developed by Melton [16] and Broucke [17]. Melton [16] used a series expansion for radial distance and true anomaly, in terms of time. However, for moderate eccentricities, the convergence of such series requires the inclusion of many higher-order terms. Inalhan et al. [18], utilizing Carter's work in [13], developed the conditions under which the TH equations admit periodic solutions.

Literature on establishing initial conditions for formations amply shows the importance of addressing the effects of eccentricity as well as nonlinearity. To this end, Anthony and Sasaki [19] obtained approximate solutions to the HCW equations by including quadratic nonlinearities and first-order eccentricity effects. Vaddi et al. [20] studied the combined problem of eccentricity and nonlinearity and obtained periodicity conditions in the presence of these effects. However, these conditions lose validity even for intermediate eccentricities, primarily because of the higher-order coupling between eccentricity and nonlinearity. Recent work by Gurfil [21] poses the bounded-motion problem in terms of the energy-matching

Presented as Paper AAS 06-162 at the 2006 AAS/AIAA Spaceflight Mechanics Meeting, Tampa, FL, January 2006; received 27 June 2005; revision received 22 December 2005; accepted for publication 2 January 2006.

*Ph.D. Candidate, Department of Aerospace Engineering; prasenjit@tamu.edu. Student Member, AIAA.

†Ph.D. Candidate, Department of Aerospace Engineering; aeroraj@tamu.edu. Student Member, AIAA.

‡Stewart & Stevenson-I Professor, Department of Aerospace Engineering; svadali@aero.tamu.edu. Associate Fellow, AIAA.

condition. Because the velocity appears in a quadratic fashion in this equation, velocity corrections to the full, nonlinear problem can be obtained in an analytical manner, without assumptions on relative orbit size. However, the more general problem of period matching is reduced to the solution of a sixth-order algebraic equation in any of the states, assuming the other five states are known. This approach requires a numerical procedure to obtain a solution, starting with an initial guess. The sixth-order polynomial has multiple roots, some of which have no physical significance. Euler and Shulman [22] first presented the TH equations perturbed by nonlinear differential gravity with no assumptions on eccentricity. However, they claimed that these equations could not be solved analytically.

Relative motion can also be characterized in a linear setting, by the use of differential orbital elements [23–28]. Because of the nonlinear mapping between local frame Cartesian coordinates and orbital elements, errors in the Cartesian frame are translated into very small errors in the orbital angles. References [23–25] approached the problem by linearizing the direction cosine matrix of the orientation of the deputy with respect to the chief. Garrison et al. [26] used true anomaly as the independent variable to obtain analytical expressions for relative motion near high-eccentricity orbits. The same objective was achieved by Sabol et al. [27], but in a time-explicit manner. In this case, a Fourier–Bessel expansion of the true anomaly in terms of the mean anomaly was used. However, for eccentricities of 0.7, terms up to the tenth order in eccentricity are required in the series. In Sengupta et al. [28], a methodology has been proposed where Kepler's equation (as cited by Battin [29]) is solved for the deputy, but is not required for the chief, if the chief's true anomaly is used as the independent variable. Although [26–28] provide accurate results for highly eccentric reference orbits, only [23–25] allow characterizing such orbital element differences in terms of the constants of the HCW solutions, viz. relative orbit size and phase. The basic zero-secular drift condition is satisfied by setting the semimajor axis of the deputy and chief to be the same. The characterization of relative orbit geometry is achieved by relating the rest of the orbital element differences to its shape, size, and the initial phase angle. Alfriend et al. [30] also introduced nonlinearities in the orbital element approach by using quadratic differential orbital elements in the geometric description of formation flight.

Though much work has been done on the problem of formation flight using orbital elements, in many ways, the use of relative motion equations in the local (rotating) Cartesian frame is preferred over orbital element differences. It is easier to obtain local ranging data directly, than to have the position and velocity of either satellite reported to a terrestrial station and translated into orbital elements. This also allows the use of decentralized control algorithms for the control of formations. Furthermore, the geometry specification in the orbital element approach followed in [23–25] assumes truncation of the eccentricity expansion to first order. For moderate or high eccentricities, this may lead to relative orbit geometry that is different from what is desired.

The work in this paper studies the perturbed TH equations by treating second-order nonlinearities. In effect, the problem posed in [22] is solved. These results are valid for arbitrary eccentricities and implicitly account for eccentricity-nonlinearity effects. The exact analytical solution, although complicated in appearance at first, leads to an elegant form of expressions for relative motion. Furthermore, the terms that lead to secular growth in the perturbed equations are easily identified as those that also lead to secular growth in the unperturbed equation, as observed in [13]. Consequently, collecting these terms and negating their effects leads to a valid condition for periodic orbits. It should be noted that this paper assumes a central gravity field without the effect of perturbations such as drag and J_2. A description of the relative motion problem in the presence of these perturbations may be found in [31].

Problem Description

Reference Frames

Consider an Earth-centered inertial (ECI) frame, denoted by $\mathcal{N}$, with orthonormal basis $\mathcal{B}_N = \{\boldsymbol{i}_x \quad \boldsymbol{i}_y \quad \boldsymbol{i}_z\}$. The vectors $\boldsymbol{i}_x$ and $\boldsymbol{i}_y$ lie in the equatorial plane, with $\boldsymbol{i}_x$ coinciding with the line of the equinoxes, and $\boldsymbol{i}_z$ passes through the North Pole. The analysis uses a local-vertical-local-horizontal (LVLH) frame, as shown in Fig. 1 and denoted by $\mathcal{L}$, that is attached to the target satellite (also called the leader or chief). This frame has basis $\mathcal{B}_L = \{\boldsymbol{i}_r \quad \boldsymbol{i}_\theta \quad \boldsymbol{i}_h\}$, with $\boldsymbol{i}_r$ lying along the radius vector from the Earth's center to the satellite, $\boldsymbol{i}_h$ coinciding with the normal to the plane defined by the position and velocity vectors of the satellite, and $\boldsymbol{i}_\theta = \boldsymbol{i}_h \times \boldsymbol{i}_r$. In this frame, the position of the chief is denoted by $\boldsymbol{r}_C = r\boldsymbol{i}_r$, where r is the radial distance, and the position of the chaser satellite (also known as the follower or deputy) is denoted by $\boldsymbol{r}_D = \boldsymbol{r}_C + \boldsymbol{\varrho}$, where $\boldsymbol{\varrho} = \xi\boldsymbol{i}_r + \eta\boldsymbol{i}_\theta + \zeta\boldsymbol{i}_h$ is the position of the deputy relative to the chief.

Equations of Motion

The equations of motion may be derived using a Lagrangian formulation, which requires the gravitational potential of the deputy:

$$V = -\frac{\mu}{|\boldsymbol{r}_D|} = -\frac{\mu}{r}\left(1 + \frac{\varrho^2}{r^2} + 2\frac{\xi}{r}\right)^{-\frac{1}{2}} \tag{1}$$

Observing that $\xi/r = (\xi/\varrho)\cdot(\varrho/r)$, the parenthesized term in the preceding equation is then the generating function for Legendre polynomials with argument $-\xi/\varrho$. Consequently

$$\begin{aligned} V &= -\frac{\mu}{r}\sum_{k=0}^{\infty}(-1)^k\left(\frac{\varrho}{r}\right)^k P_k(\xi/\varrho) \\ &= -\frac{\mu}{r}\left[1 - \frac{\xi}{r} + \frac{1}{2}\frac{(2\xi^2 - \eta^2 - \zeta^2)}{r^2}\right] + \tilde{V} \end{aligned} \tag{2}$$

$$\tilde{V} = -\frac{\mu}{r}\sum_{k=3}^{\infty}(-1)^k\left(\frac{\varrho}{r}\right)^k P_k(\xi/\varrho) \tag{3}$$

where P_k is the kth Legendre polynomial. Consequently, the equations of motion are

$$\ddot{\xi} - 2\dot{\theta}\dot{\eta} - \left(\dot{\theta}^2 + 2\frac{\mu}{r^3}\right)\xi - \ddot{\theta}\eta = -\frac{\partial\tilde{V}}{\partial\xi} \tag{4a}$$

$$\ddot{\eta} + 2\dot{\theta}\dot{\xi} - \left(\dot{\theta}^2 - \frac{\mu}{r^3}\right)\eta + \ddot{\theta}\xi = -\frac{\partial\tilde{V}}{\partial\eta} \tag{4b}$$

$$\ddot{\zeta} + \frac{\mu}{r^3}\zeta = -\frac{\partial\tilde{V}}{\partial\zeta} \tag{4c}$$

where θ is the argument of latitude given by $\theta = \omega + f$, with ω denoting the argument of periapsis and f the true anomaly. Also

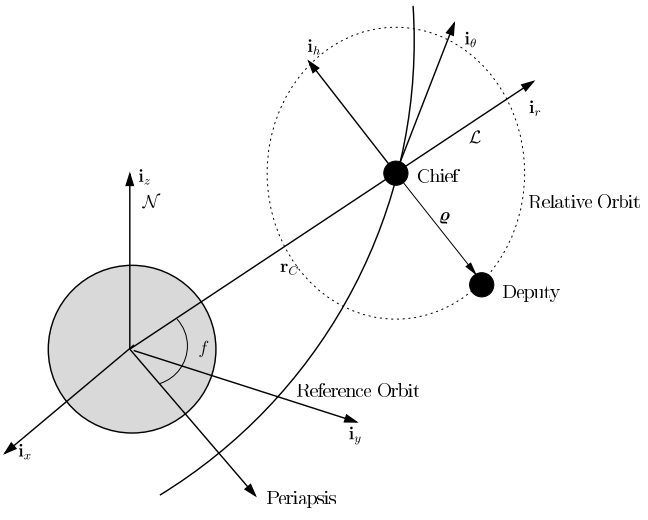

Fig. 1 Frames of reference.

useful are the equations for the radius and the argument of latitude [29]:

$$\ddot{r} = \dot{\theta}^2 r - \frac{\mu}{r^2} \tag{5a}$$

$$\ddot{\theta} = -2\frac{\dot{r}}{r}\dot{\theta} \tag{5b}$$

Higher-order Legendre polynomials in the perturbing potential can be generated from lower-order ones, by using the recursive relation $(k+1)P_{k+1}(z) = (2k+1)zP_k(z) - kP_{k-1}(z)$, with $P_0(z) = 1$ and $P_1(z) = z$. The perturbing gravitational acceleration $\partial\tilde{V}/\partial\boldsymbol{\varrho} = \{\partial\tilde{V}/\partial\xi \quad \partial\tilde{V}/\partial\eta \quad \partial\tilde{V}/\partial\zeta\}^T$ contributes higher-order nonlinearities to the system, and if ignored, allows the treatment of Eq. (4) as a tenth-order linear system (additional equations are contributed by Keplerian motion). This can be converted to a sixth-order linear system with periodic coefficients, if the independent variable is changed from t to f. Use is made of the formulas $\dot{f} = h/r^2$, where the angular momentum $h = \sqrt{\mu a(1-e^2)}$ and $r = a(1-e^2)/(1+e\cos f)$, with semimajor axis a and eccentricity e. Consequently

$$(\dot{}) = \dot{f}(') = \bar{n}(1+e\cos f)^2(') \tag{6a}$$

$$\begin{aligned}(\ddot{}) &= \dot{f}^2('') + \ddot{f}(') \\ &= \bar{n}^2(1+e\cos f)^3[(1+e\cos f)('') - 2e\sin f(')]\end{aligned} \tag{6b}$$

where $(')$ denotes the derivative with respect to f, $\bar{n} = n/(1-e^2)^{3/2}$, and $n = \sqrt{(\mu/a^3)}$ is the mean motion.

To calculate the perturbing differential gravitational acceleration $\partial\tilde{V}/\partial\boldsymbol{\varrho}$, the following relation is made use of:

$$\frac{\mathrm{d}}{\mathrm{d}z}P_k(z) = \frac{k}{z^2-1}[zP_k(z) - P_{k-1}(z)] \tag{7}$$

Using $\varrho^2 = \xi^2 + \eta^2 + \zeta^2$, and $\partial\xi/\partial\boldsymbol{\varrho} = \boldsymbol{i}_r$, it can be shown that

$$\begin{aligned}\frac{\partial\tilde{V}}{\partial\boldsymbol{\varrho}} &= -\frac{\mu}{r^3}\sum_{k=3}^{\infty}(-1)^k\left(\frac{\varrho}{r}\right)^{k-2}\frac{k}{\eta^2+\zeta^2}[\varrho^2 P_k(\xi/\varrho)\boldsymbol{i}_1 \\ &\quad + \varrho P_{k-1}(\xi/\varrho)\boldsymbol{i}_2]\end{aligned} \tag{8}$$

where $\boldsymbol{i}_1 = \eta\boldsymbol{i}_\theta + \zeta\boldsymbol{i}_h$ and $\boldsymbol{i}_2 = (\eta^2+\zeta^2)\boldsymbol{i}_r - \xi\eta\boldsymbol{i}_\theta - \xi\zeta\boldsymbol{i}_h$. Upon resolution, the perturbing differential gravity field can be rewritten as a series involving the following small, dimensionless parameter:

$$\epsilon = \frac{\varrho_0}{a(1-e^2)} \tag{9}$$

where ϱ_0 is some measure of the relative orbit size. For low eccentricities, this may be the circular orbit radius as predicted by the HCW solutions. Without loss of generality, $\varrho_0 = \sqrt{(\xi_0^2+\eta_0^2+\zeta_0^2)} \ll a$. The expression for the perturbed gravitational acceleration, along with Eq. (6), is now used in Eq. (4). Furthermore, the system of equations is divided by $\bar{n}^2(1+e\cos f)^4$ that appears on both sides of the equation. A nondimensional position vector $\boldsymbol{\rho} = x\boldsymbol{i}_r + y\boldsymbol{i}_\theta + z\boldsymbol{i}_h$ is introduced. This vector is obtained from $\boldsymbol{\varrho}$ by nondimensionalizing it with respect to ϱ_0, and by the following transformation [8,12]:

$$\boldsymbol{\rho} = \frac{\boldsymbol{\varrho}}{\varrho_0}(1+e\cos f) \tag{10}$$

Consequently,

$$\boldsymbol{\rho}' = \frac{\boldsymbol{\varrho}'}{\varrho_0}(1+e\cos f) - \frac{\boldsymbol{\varrho}}{\varrho_0}e\sin f \tag{11a}$$

$$\boldsymbol{\rho}'' = \frac{\boldsymbol{\varrho}''}{\varrho_0}(1+e\cos f) - 2\frac{\boldsymbol{\varrho}'}{\varrho_0}e\sin f - \frac{\boldsymbol{\varrho}}{\varrho_0}e\cos f \tag{11b}$$

The complete equations of motion are as follows:

$$\begin{aligned}&\begin{Bmatrix}x''\\y''\\z''\end{Bmatrix} + \begin{bmatrix}0&-2&0\\2&0&0\\0&0&0\end{bmatrix}\begin{Bmatrix}x'\\y'\\z'\end{Bmatrix} \\ &\quad + \begin{bmatrix}-3/(1+e\cos f)&0&0\\0&0&0\\0&0&1\end{bmatrix}\begin{Bmatrix}x\\y\\z\end{Bmatrix} \\ &\quad = \sum_{k=3}^{\infty}\frac{\epsilon^{k-2}(-1)^k k}{(1+e\cos f)(y^2+z^2)} \\ &\quad \times\left[\rho^k P_k(x/\rho)\begin{Bmatrix}0\\y\\z\end{Bmatrix} + \rho^{k-1}P_{k-1}(x/\rho)\begin{Bmatrix}y^2+z^2\\-xy\\-xz\end{Bmatrix}\right] \\ &\quad = \epsilon\frac{3}{2}(1+e\cos f)^{-1}\begin{Bmatrix}y^2+z^2-2x^2\\2xy\\2xz\end{Bmatrix} + \mathcal{O}(\epsilon^2)\end{aligned} \tag{12}$$

From Eq. (12), it is evident that if the terms of order ϵ and higher are ignored, then the equations reduce to the unperturbed Tschauner–Hempel equations. Additionally, if $e = 0$, then the HCW equations are obtained. It should be noted that the small parameter ϵ depends not only on the size of the relative orbit, but also on the eccentricity of the reference. This reflects the fact that eccentricity and nonlinearity effects in formation flight are coupled.

Solution Using a Perturbation Approach

A straightforward expansion [32] of the following form is considered

$$\begin{aligned}x(f) = x_0(f) + \epsilon x_1(f) + \cdots, \qquad y(f) = y_0(f) + \epsilon y_1(f) + \cdots \\ z(f) = z_0(f) + \epsilon z_1(f) + \cdots\end{aligned} \tag{13}$$

Lindstedt–Poincaré or renormalization techniques are not required because a frequency correction is not necessary. In a central gravity field, periodic motion between two satellites is only possible when the two satellites have the same mean motion. Consequently, the frequency of the relative orbit is the same as that of the orbits of either satellite. It will be shown that the most general solution for bounded orbits of the TH equations, without perturbations (zeroth-order equations), has the same frequency as the orbital period of each satellite. Consequently, higher-order corrections to the frequency must necessarily be zero, because the coefficient corresponding to each correction is an increasing power of the small parameter.

Equation (13) is substituted in Eq. (12), with perturbations up to order ϵ included. Collecting terms of the same order, the following two systems are obtained:

$$x_0'' - 2y_0' - \frac{3x_0}{(1+e\cos f)} = 0 \tag{14a}$$

$$y_0'' + 2x_0' = 0 \tag{14b}$$

$$z_0'' + z_0 = 0 \tag{14c}$$

and

$$x_1'' - 2y_1' - \frac{3x_1}{(1+e\cos f)} = \frac{3}{2}\frac{(y_0^2+z_0^2-2x_0^2)}{(1+e\cos f)} \tag{15a}$$

$$y_1'' + 2x_1' = \frac{3x_0y_0}{(1+e\cos f)} \tag{15b}$$

$$z_1'' + z_1 = \frac{3x_0 z_0}{(1 + e\cos f)} \tag{15c}$$

Solution to the Unperturbed System

The approach followed in this section is for epoch at a general initial value of true anomaly f_i. In a later section, the explicit formulation for $f_i = 0$ (periapsis) and $f_i = \pi$ (apoapsis) will be presented. This considerably simplifies the expressions obtained.

It can be shown that the solution to the homogeneous zeroth-order system given by Eq. (14) is [12,13]

$$x_0(f) = c_1\cos f(1 + e\cos f) + c_2\sin f(1 + e\cos f) + c_3\left[2e\sin f(1 + e\cos f)H(f) - \frac{\cos f}{(1 + e\cos f)}\right] \tag{16a}$$

$$y_0(f) = -c_1\sin f(2 + e\cos f) + c_2\cos f(2 + e\cos f) + 2c_3(1 + e\cos f)^2 H(f) + c_4 \tag{16b}$$

$$z_0(f) = c_5\cos f + c_6\sin f \tag{16c}$$

$$x_0'(f) = -c_1(\sin f + e\sin 2f) + c_2(\cos f + e\cos 2f) + c_3\left[2e(\cos f + e\cos 2f)H(f) + \frac{(\sin f + e\sin 2f)}{(1 + e\cos f)^2}\right] \tag{16d}$$

$$y_0'(f) = -c_1(2\cos f + e\cos 2f) - c_2(2\sin f + e\sin 2f) - 2c_3\left[e(2\sin f + e\sin 2f)H(f) - \frac{\cos f}{(1 + e\cos f)}\right] \tag{16e}$$

$$z_0'(f) = -c_5\sin f + c_6\cos f \tag{16f}$$

where $H(f)$ is a function evaluated in terms of the eccentric anomaly E [13]:

$$H(f) = \int \frac{\cos f}{(1 + e\cos f)^3}\,\mathrm{d}f = -(1 - e^2)^{-5/2} \times \left[\frac{3e}{2}E - (1 + e^2)\sin E + \frac{e}{4}\sin 2E\right] \tag{17}$$

The following equations relate the eccentric and true anomalies [29]:

$$\cos f = \frac{\cos E - e}{1 - e\cos E}, \qquad \sin f = \frac{(1 - e^2)^{1/2}\sin E}{1 - e\cos E}$$
$$\cos E = \frac{\cos f + e}{1 + e\cos f}, \qquad \sin E = \frac{(1 - e^2)^{1/2}\sin f}{1 + e\cos f}$$

It is shown in [33] that a first-order periodicity condition can easily be derived by studying Eq. (16). Let the initial conditions for the zeroth-order (unperturbed) system be denoted by the vector $\boldsymbol{x}_{0_i} = \{x_{0_i} \quad y_{0_i} \quad z_{0_i} \quad x'_{0_i} \quad y'_{0_i} \quad z'_{0_i}\}^T$, specified at arbitrary initial true anomaly f_i, and let the vector of integration constants be denoted by $\boldsymbol{c} = \{c_1 \cdots c_6\}^T$, the relation $\boldsymbol{x}_{0_i} = \mathbf{L}\boldsymbol{c}$ holds. The entries of matrix $\mathbf{L}$, denoted by L_{jk}, $j = 0\ldots6$, $k = 0\ldots6$, are constructed by substituting f_i in the right hand side of Eq. (16). From the structure of Eqs. (16) and (17), it is observed that secular growth is contributed by those terms with coefficient c_3. This is also observed in [18]. Consequently, the generalized condition for periodicity [33] is

$$l_1 x_{0_i} + l_2 x'_{0_i} + l_3 y'_{0_i} = 0 \tag{18}$$

where

$$l_1 = L_{52}L_{41} - L_{51}L_{42} = e^2 + 3e\cos f_i + 2$$
$$l_2 = L_{12}L_{51} - L_{11}L_{52} = e\sin f_i(1 + e\cos f_i)$$
$$l_3 = L_{42}L_{11} - L_{41}L_{12} = (1 + e\cos f_i)^2$$

This condition is satisfied for infinite combinations of initial conditions, and for resolution, a constraint is required. One suitable constraint may be to keep the initial states as a given and calculate the minimum velocity impulse required to obtain a periodic orbit. A similar approach has been used in [18], wherein the Δv for formation insertion is minimized by posing the problem as a linear program. The problem may also be posed as one where the 2-norm of the impulse, with components $\Delta x'_0$ and $\Delta y'_0$, is minimized:

$$\min \Phi(\Delta x'_0, \Delta y'_0) = (\Delta x_0'^2 + \Delta y_0'^2)^{1/2}$$

subject to

$$\Psi(\Delta x'_0, \Delta y'_0) = l_1 x_{0_i} + l_2(x'_{0_i} + \Delta x'_0) + l_3(y'_{0_i} + \Delta y'_0) = 0 \tag{19}$$

By minimizing $\Phi + \lambda\Psi$, where λ is a Lagrange multiplier, the following unique solution is obtained:

$$\Delta x'_0 = -\frac{l_2}{l_{22} + l_{32}}(l_1 x_{0_i} + l_2 x'_{0_i} + l_3 y'_{0_i}) \tag{20a}$$

$$\Delta y'_0 = -\frac{l_3}{l_2^2 + l_3^2}(l_1 x_{0_i} + l_2 x'_{0_i} + l_3 y'_{0_i}) \tag{20b}$$

Irrespective of the manner in which the initial conditions are established, as long as $c_3 = 0$, the most general periodic solution to the TH equations may be rewritten as [33]

$$x_p(f) = \rho_1\sin(f + \alpha)(1 + e\cos f) \tag{21a}$$

$$y_p(f) = \rho_1\cos(f + \alpha)(2 + e\cos f) + \rho_2 \tag{21b}$$

$$z_p(f) = \rho_3\sin(f + \beta) \tag{21c}$$

where the subscript p denotes a periodic relative orbit. The relative orbit parameters ρ_1 and ρ_3 indicate relative orbit size, ρ_2 introduces a bias in along-track motion, and the angles α and β indicate the phase of the deputy. These relative orbit parameters may be obtained from the integration constants, by the following:

$$\rho_1 = (c_1^2 + c_2^2)^{1/2}, \qquad \rho_2 = c_4, \qquad \rho_3 = (c_5^2 + c_6^2)^{1/2} \tag{22a}$$

$$\alpha = \tan^{-1}\left(\frac{c_1}{c_2}\right), \qquad \beta = \tan^{-1}\left(\frac{c_5}{c_6}\right) \tag{22b}$$

If $e = 0$, then the solutions are the same as those for the HCW equations. It is now evident that circular orbits in the fashion of HCW projected circular orbit or general circular orbit cannot be obtained if $e \neq 0$.

Solution to the Perturbed System

Having obtained initial conditions for periodicity in the unperturbed system, its periodic form is now substituted in Eq. (15). The solutions to these equations are similar to Eq. (16), with additional particular integrals. The equation in $z_1(f)$ is considered separately, due to its tractable nature:

$$z_1'' + z_1 = \frac{3x_p z_p}{(1 + e\cos f)} = 3\rho_1\rho_3\sin(f + \alpha)\sin(f + \beta) \tag{23}$$

Solving Eq. (23) yields

$$z_1(f) = k_1\cos f + k_2\sin f + \tfrac{1}{2}\rho_1\rho_3[3\cos(\alpha - \beta) + \cos(2f + \alpha + \beta)] \tag{24}$$

Because there are no secular growth terms in Eq. (24), an arbitrary choice may be made for the constants of integration k_1 and k_2. To remove terms with $\cos(f)$ and $\sin(f)$, that is, to ensure that the mean value of the z amplitude is the same as that predicted by the linear equations, the following choices for the initial conditions are made:

$$z_{1_i} = \tfrac{1}{2}\rho_1\rho_3\cos(2f_i + \alpha + \beta) + \tfrac{3}{2}\rho_1\rho_3\cos(\alpha - \beta) \tag{25a}$$

$$z'_{1_i} = -\rho_1\rho_3\sin(2fi + \alpha + \beta) \tag{25b}$$

As a result,

$$z_1(f) = \tfrac{3}{2}\rho_1\rho_3\cos(\alpha - \beta) + \tfrac{1}{2}\rho_1\rho_3\cos(2f + \alpha + \beta) \tag{26}$$

Carter and Humi [12] develop the TH equations in the presence of a forcing function. Utilizing this result, it can be shown that the x_1 and y_1 solutions are

$$\begin{aligned} x_1(f) &= b_1\cos f(1 + e\cos f) + b_2\sin f(1 + e\cos f) \\ &\quad + b_3\left[2e\sin f(1 + e\cos f)H(f) - \frac{\cos f}{(1 + e\cos f)}\right] \\ &\quad + \phi\int\frac{L}{\phi^2}\,\mathrm{d}f \end{aligned} \tag{27a}$$

$$\begin{aligned} y_1(f) &= -b_1\sin f(2 + e\cos f) + b_2\cos f(2 + e\cos f) \\ &\quad + 2b_3(1 + e\cos f)^2H(f) + b_4 + 3\iint\frac{x_p y_p}{(1 + e\cos f)}\,\mathrm{d}f \\ &\quad + \frac{1}{e}\left[(1 + e\cos f)^2\int\frac{L}{\phi^2}\,\mathrm{d}f - \int\frac{L}{\sin^2 f}\,\mathrm{d}f\right]\prod \end{aligned} \tag{27b}$$

where $\phi = \sin f(1 + e\cos f)$, and

$$\begin{aligned} L &= \frac{3}{2}\int(y_p^2 + z_p^2 - 2x_p^2)\sin f\,\mathrm{d}f - \frac{3}{e}(1 + e\cos f)^2 \\ &\quad \times\int\frac{x_p y_p}{(1 + e\cos f)}\,\mathrm{d}f + \frac{3}{e}\int x_p y_p(1 + e\cos f)\,\mathrm{d}f \\ &= L_0 + \sum_{k=1}^{5}(L_{c_k}\cos kf + L_{s_k}\sin kf) \end{aligned} \tag{28}$$

The coefficients $\{L_0, L_{c_1}\cdots L_{c_5}, L_{s_1}\cdots L_{s_5}\}$ are provided in the Appendix. The complete solution of Eq. (27) requires the evaluation of the integrals of $\cos(kf)/\phi^2$, $\sin(kf)/\phi^2$, $\cos(kf)/\sin^2 f$, and $\sin(kf)/\sin^2 f$, $k = 1\ldots5$. These integrals can also be evaluated in terms of $H(f)$ and sinusoidal functions of the true anomaly, and are presented in the Appendix. Though it may appear that the terms in the Appendix are not defined for $f = n\pi$, it should be noted that when multiplied by the appropriate coefficient, the logarithmic terms, and terms containing f explicitly, cancel each other, and are therefore ignored from further analysis. Consequently, the analytical solution to the perturbed system can be constructed.

From the Appendix and the solution to Eq. (27a), the secular growth terms are identified as those that contain $H(f)$. It follows that setting the combined coefficient of $H(f)$ to zero will prevent secular growth to the second order. Collecting the coefficients of $H(f)$ in $x_1(f)$ results in the following condition:

$$\begin{aligned} &2eb_3 + 2eL_0 - \frac{2}{3}(2 + e^2)L_{c_1} + \frac{2}{3e}(2 + e^2)L_{c_2} - 2(2 - e^2)L_{c_3} \\ &\quad - \frac{2}{3e^3}(8 - 24e^2 + 13e^4)L_{c_4} - \frac{2}{3e^4}(32 - 80e^2 \\ &\quad + 50e^4 - 5e^6)L_{c_5} = 0 \end{aligned} \tag{29}$$

or

$$\begin{aligned} b_3 &= -\frac{e}{4}(2\rho_1^2\cos 2\alpha + \rho_3^2\cos 2\beta) - 2\rho_1\rho_2\cos\alpha \\ &\quad - \frac{e}{4}(\rho_1^2 + 2\rho_2^2 + \rho_3^2) - \frac{1}{2e}(2\rho_1^2 + 2\rho_2^2 + \rho_3^2) \end{aligned} \tag{30}$$

The seemingly complex integrals involved in the equation actually reduce to fairly simple expressions. Ignoring the terms containing $H(f)$, because they are rendered absent by the choice of b_3 in Eq. (30), the integrals may be rewritten as the following:

$$p_1(f) = \phi\int\frac{L}{\phi^2}\,\mathrm{d}f = \sum_{k=1}^{3}G_k\sin kf + \frac{1}{(1 + e\cos f)}\sum_{k=0}^{4}H_k\cos kf \tag{31a}$$

$$q_1(f) = 3\iint\frac{x_p y_p}{(1 + e\cos f)}\,\mathrm{d}f = \sum_{k=1}^{3} = (E_k\sin kf + F_k\cos kf) \tag{31b}$$

$$\begin{aligned} q_2(f) &= \frac{1}{e}\left[(1 + e\cos f)^2\int\frac{L}{\phi^2}\,\mathrm{d}f - \int\frac{L}{\sin^2 f}\,\mathrm{d}f\right] \\ &= D_0 + \sum_{k=1}^{3}(C_k\sin kf + D_k\cos kf) \end{aligned} \tag{31c}$$

The coefficients are presented in the Appendix.

The initial conditions for the perturbed system $\boldsymbol{x}_{1_i} = \{x_{1_i} \quad y_{1_i} \quad x'_{1_i} \quad y'_{1_i}\}^T$, integration constants $\boldsymbol{b} = \{b_1\cdots b_4\}^T$, and initial values of the forcing function, are related by the following:

$$\boldsymbol{x}_{1_i} = \tilde{\mathbf{L}}\boldsymbol{b} + \boldsymbol{w} \tag{32}$$

It follows that

$$\tilde{\mathbf{L}} = \begin{bmatrix} L_{11} & L_{12} & L_{13} & 0 \\ L_{21} & L_{22} & L_{23} & 1 \\ L_{41} & L_{42} & L_{43} & 0 \\ L_{51} & L_{52} & L_{53} & 0 \end{bmatrix} \tag{33}$$

It is shown in [33] that $\det\tilde{\mathbf{L}} = L_{13}l_1 + L_{43}l_2 + L_{53}l_3 = 1$. The initial values of the forcing functions are given by $\boldsymbol{w} = \{p_1 \ (q_1 + q_2) \ p'_1 \ (-2p_1 + q'_1)\}^T$ evaluated at $f = f_i$.

Initial conditions are required that will lead to the particular value of b_3 specified in Eq. (30). This provides one constraint on the initial conditions. If only a velocity correction is required, one may choose $x_{1_i} = y_{1_i} = x'_{1_i} = 0$. By substituting the $b_{1\ldots3}$ obtained from solving Eq. (32) into the last equation for y'_{1_i}, the following is obtained:

$$\begin{aligned} y'_{1_i} &= \frac{l_1}{l_3}(p_1 + L_{13}b_3) + \frac{l_2}{l_3}(p'_1 + L_{43}b_3) + L_{53}b_3 - 2p_1 + q'_1 \\ &= -\frac{e(\cos f_i + e\cos 2f_i)}{(1 + e\cos f_i)^2}p_1 + \frac{e\sin f_i}{(1 + e\cos f_i)}p'_1 + q'_1 \\ &\quad + \frac{eb_3}{(1 + e\cos f_i)^2} = \Delta \end{aligned} \tag{34}$$

It should be noted that the apparent zero-eccentricity singularity in Eq. (30) is removed by the e multiplier in Eq. (34). The quantity Δ specifies the correction to the initial conditions required to negate secular growth arising from second-order differential gravity. Consequently,

$$\Delta x' = -\frac{l_2}{l_2^2 + l_3^2}[l_1 x(f_i) + l_2 x'(f_i) + l_3 y'(f_i)] \tag{35a}$$

$$\Delta y' = -\frac{l_3}{l_2^2 + l_3^2}[l_1 x(f_i) + l_2 x'(f_i) + l_3 y'(f_i)] + \epsilon\Delta \tag{35b}$$

To convert this to initial relative position and velocity, $(\xi_i, \eta_i, \zeta_i, \dot{\xi}_i, \dot{\eta}_i, \dot{\zeta}_i)$ with time as the independent variable, the

following transformation may be used:

$$\begin{Bmatrix} \xi_i \\ \eta_i \\ \zeta_i \end{Bmatrix} = \frac{\varrho_0}{(1+e\cos f_i)} \begin{Bmatrix} x_i \\ y_i \\ z_i \end{Bmatrix} \tag{36a}$$

$$\begin{Bmatrix} \dot{\xi}_i \\ \dot{\eta}_i \\ \dot{\zeta}_i \end{Bmatrix} = \varrho_0 \bar{n}(1+e\cos f_i) \begin{Bmatrix} x_i' \\ y_i' \\ z_i' \end{Bmatrix} + \varrho_0 \bar{n}(e\sin f_i) \begin{Bmatrix} x_i \\ y_i \\ z_i \end{Bmatrix} \tag{36b}$$

Time itself can be obtained from the direct solution to Kepler's equation:

$$t = \frac{1}{n}(E - e\sin E) \tag{37}$$

Epoch at Periapsis/Apoapsis

The expressions are simplified greatly if it is assumed that $f_i = 0$ or $f_i = \pi$. At these values of f_i, $l_2 = 0$. The condition for periodicity in the linearized field reduces to

$$y_{0_i}' = -\frac{(2 \pm e)}{(1 \pm e)} x_{0_i} \tag{38}$$

where the positive and negative signs denote $f_i = 0$ and $f_i = \pi$, respectively. These are obtained in an equivalent fashion in [18]. Because $l_2 = 0$, it is now unnecessary to evaluate p_1'. From the expressions for L_0, L_{c_k}, and L_{s_k} that are presented in the Appendix, it is observed that

$$\begin{aligned} p_1(0) &= -\frac{1}{(1+e)}\left(L_0 + \sum_{k=1}^{5} L_{c_k}\right) \\ &= \frac{1}{(1+e)}\left[\frac{1}{4}\rho_3^2\cos 2\beta - \frac{1}{4}\rho_1^2(5e + e^2 + 2)\cos 2\alpha \right. \\ &\left. - \rho_1\rho_2(3+e)\cos\alpha + \frac{3}{2}\rho_1^2 - \frac{1}{4}\rho_1^2 e^2 + \frac{3}{4}\rho_3^2 + \frac{3}{2}\rho_2^2\right] \end{aligned} \tag{39a}$$

$$\begin{aligned} p_1(\pi) &= \frac{1}{(1-e)}\left(L_0 + \sum_{k=1}^{5}(-1)^k L_{c_k}\right) \\ &= \frac{1}{(1-e)}\left[\frac{1}{4}\rho_3^2\cos 2\beta - \frac{1}{4}\rho_1^2(-5e + e^2 + 2)\cos 2\alpha \right. \\ &\left. + \rho_1\rho_2(3-e)\cos\alpha + \frac{3}{2}\rho_1^2 - \frac{1}{4}\rho_1^2 e^2 + \frac{3}{4}\rho_3^2 + \frac{3}{2}\rho_2^2\right] \end{aligned} \tag{39b}$$

By substituting p_1, $q_1' = E_1 + 2E_2 + 3E_3$, and b_3 in Eq. (34), the initial condition correction is

$$\begin{aligned} y_{1_i}' &= \frac{1}{4}\frac{(e^2 \mp 2e - 4)\rho_1^2}{1 \pm e} - \frac{1}{4}\frac{(2 \pm e)}{(1 \pm e)}(2\rho_2^2 + \rho_3^2) \mp \frac{1}{4}\frac{e\rho_3^2\cos 2\beta}{1 \pm e} \\ &- \frac{1}{4}\frac{\rho_1^2(3e^2 \pm 8e + 6)\cos 2\alpha}{1 \pm e} - \frac{\rho_1\rho_2(2e \pm 3)\cos\alpha}{1 \pm e} \end{aligned} \tag{40}$$

Second-Order Analytical Expressions for Relative Motion

Because the choice of the constants b_1, b_2, and b_4 is arbitrary, they may be chosen to yield a suitable second-order equation for relative motion. Equation (27b) is now reconsidered. Upon substituting Eq. (30) in Eq. (27b), it can be shown that

$$\begin{aligned} y_1(f) &= (-2b_1 + C_1 + E_1)\sin f + \left(-\frac{eb_1}{2} + C_2 + E_2\right)\sin 2f \\ &+ (C_3 + E_3)\sin 3f + (2b_2 + D_1 + F_1)\cos f \\ &+ \left(\frac{eb_2}{2} + D_2 + F_2\right)\cos 2f + (D_3 + F_3)\cos 3f \\ &+ \left(\frac{eb_2}{2} + b_4 + D_0\right) \end{aligned} \tag{41}$$

It is observed that $C_3 = -E_3$ and $D_3 = -F_3$. The values of b_1, b_2, and b_4 can be chosen such that the coefficients of $\sin f$ and $\cos f$ and the constant term are zero. In this event,

$$b_1 = \tfrac{1}{2}(C_1 + E_1) \tag{42a}$$

$$b_2 = -\tfrac{1}{2}(D_1 + F_1) \tag{42b}$$

$$b_4 = -D_0 - \frac{eb_2}{2} \tag{42c}$$

Consequently,

$$\begin{aligned} y_1(f) &= \left(-\frac{eC_1}{4} - \frac{eE_1}{4} + C_2 + E_2\right)\sin 2f + \left(-\frac{eD_1}{4} - \frac{eF_1}{4}\right. \\ &\left. + D_2 + F_2\right)\cos 2f \\ &= -\frac{e^2}{8}\rho_1^2\sin 2f + \frac{e}{4}\rho_1\rho_2\sin(2f+\alpha) - \frac{1}{8}(2-e^2)\rho_1^2 \\ &\times \sin(2f + 2\alpha) - \frac{1}{4}\rho_3^2\sin(2f + 2\beta) \end{aligned} \tag{43}$$

Now Eq. (27a) is considered, after the removal of secular terms. In this case,

$$\begin{aligned} x_1(f) &= b_1\cos f(1 + e\cos f) + b_2\sin f(1 + e\cos f) \\ &+ G_1\sin f + G_2\sin 2f + G_3\sin 3f + \frac{1}{(1 + e\cos f)} \\ &\times [H_0 + (H_1 - b_3)\cos f + H_2\cos 2f \\ &+ H_3\cos 3f + H_4\cos 4f] \end{aligned} \tag{44}$$

It can be shown that

$$\begin{aligned} &\frac{1}{(1 + e\cos f)}[H_0 + (H_1 - b_3)\cos f + H_2\cos 2f + H_3\cos 3f \\ &+ H_4\cos 4f] \\ &= N_1\cos f + N_2\cos 2f + N_3\cos 3f \end{aligned} \tag{45}$$

where $N_1 = -C_1/2$, $N_2 = -C_2$, and $N_3 = -3C_3/2$. It follows that

$$\begin{aligned} x_1(f) &= \frac{eb_1}{2} + (b_1 + N_1)\cos f + (b_2 + G_1)\sin f \\ &+ \left(\frac{eb_1}{2} + N_2\right)\cos 2f + \left(\frac{eb_2}{2} + G_2\right)\sin 2f + N_3\cos 3f \\ &+ G_3\cos 3f \\ &= -\frac{1}{8}[(4 - e^2)\rho_1^2 + 4\rho_2^2 + 2\rho_3^2] - \frac{e}{4}\rho_1\rho_2\cos\alpha \\ &- \frac{e^2}{8}\rho_1^2\cos 2\alpha - \frac{3}{2}\rho_1\rho_2\cos(f+\alpha) - \frac{3e}{8}\rho_1^2\cos(f+2\alpha) \\ &- \frac{e}{4}\rho_1\rho_2\cos(2f+\alpha) + \frac{e^2}{8}\rho_1^2\cos 2f - \frac{1}{8}(4 + e^2) \\ &\times \rho_1^2\cos(2f + 2\alpha) + \frac{1}{4}\rho_3^2\cos(2f + 2\beta) \\ &- \frac{e}{8}\rho_1^2\cos(3f + 2\alpha) \end{aligned} \tag{46}$$

The analytical solution for a relative orbit near a Keplerian orbit, accounting for second-order terms, is thus given by Eq. (13) with $x_0(f), y_0(f); z_0(f)$ given by Eq. (21); and $x_1(f), y_1(f)$, and $z_1(f)$ by Eqs. (46), (43), and (24), respectively.

Periodic Orbits and the Energy-Matching Condition

Two spacecraft in Keplerian elliptic orbits will have periodic relative motion if the total energy $\mathcal{E}$ of each spacecraft (and consequently, the semimajor axis of each spacecraft) is the same. Denoting the quantities of the deputy with subscript D and those of the chief with subscript C, the vis-viva equation [29] for each spacecraft leads to the following condition for periodic relative motion:

$$\Delta\mathcal{E}(\xi,\eta,\zeta,\dot{\xi},\dot{\eta},\dot{\zeta}) \triangleq \mathcal{E}_D - \mathcal{E}_C = -\left(\frac{\mu}{2a_D} - \frac{\mu}{2a_c}\right) = \left(\frac{v_D^2}{2} - \frac{\mu}{r_D}\right) - \left(\frac{v_C^2}{2} - \frac{\mu}{r_C}\right) = 0 \tag{47}$$

Using $\mathbf{r}_D = (r+\xi)\boldsymbol{i}_r + \eta\boldsymbol{i}_\theta + \zeta\boldsymbol{i}_h$ and $\mathbf{v}_D = (\dot{r}+\dot{\xi}-\dot{\theta}\eta)\boldsymbol{i}_r + (\dot{\eta}+\dot{\theta}\xi+\dot{\theta}r)\boldsymbol{i}_\theta + \dot{\zeta}\boldsymbol{i}_h$, and normalizing these quantities in the same manner as that in the previous sections, Eq. (47) can be rewritten as

$$\begin{aligned}\Delta\mathcal{E}(\boldsymbol{\rho},\boldsymbol{\rho}') &= \frac{(2+3ec_f+e^2)}{(1+ec_f)}x + es_f x' + (1+ec_f)y' \\ &+ \frac{\epsilon}{2(1+ec_f)}[-(1-e^2)x^2 + (2+3ec_f+e^2)y^2 \\ &+ (1+ec_f+e^2s_f^2)z^2 + (1+ec_f)^2(x'^2+y'^2+z'^2) \\ &+ 2es_f(1+ec_f)(xx'+yy'+zz') + 2(1+ec_f)^2(xy'-yx')] \\ &+ \sum_{n=2}^{\infty}(-1)^n\epsilon^n\rho^{n+1}P_{n+1}\left(\frac{x}{\rho}\right) = 0\end{aligned} \tag{48}$$

where c_f and s_f denote the cosine and sine of f, respectively. If terms of $\mathcal{O}(\epsilon)$ and higher are neglected, then Eq. (48) is exactly the same as Eq. (18). Appending the correction scheme developed in this paper to the initial conditions leads to $\Delta\mathcal{E}(\boldsymbol{\rho},\boldsymbol{\rho}') = \mathcal{O}(\epsilon^2)$. This may be observed by using Eq. (40) and setting $f = 0$ in Eq. (48). Consequently,

$$\Delta\mathcal{E} \approx \frac{\mu}{2a^2}\Delta a \approx \varrho_0 a(1-e^2)\bar{n}^2\epsilon^2 \tag{49a}$$

$$\Delta a = \frac{2\varrho_0^3}{a^2(1-e^2)^4} \tag{49b}$$

The effect of eccentricity on the semimajor axis difference is thus clearly evident.

The formation-keeping problem may be posed by appending $\Delta\mathcal{E}(\boldsymbol{\rho},\boldsymbol{\rho}') = 0$ as a constraint to a cost function comprising velocity increments. In [21] it is shown that instead of expanding the period-matching condition in terms of Legendre polynomials, the velocity increments can be solved for the complete nonlinear system analytically. This is possible because the relative velocity terms appear only up to the second order in Eq. (48).

Drift Measurement

To measure the efficacy of the initial condition corrections developed in this paper, an index is desired that captures secular drift and periodic motion behavior. Unlike the solutions to the linear, autonomous HCW equations, circular relative orbits in the general elliptic case cannot be obtained. Consequently, a new measure of deviation from the nominal solution is desired, which can be used to compare the results in this paper, with existing results in the literature. Therefore, the following measure of error is defined:

$$\delta(t) \triangleq \left[\frac{1}{t}\int_0^t [\rho(t) - \rho_p(t)]^2\,\mathrm{d}t\right]^{1/2} \tag{50}$$

where $\rho = \sqrt{(x^2+y^2+z^2)}$ and $\rho_p = \sqrt{(x_p^2+y_p^2+z_p^2)}$. The advantage of using this function is in its behavior in the presence of various forms of error. Phase, frequency, or amplitude errors lead to a constant value of $\delta(t)$ as t increases, as can be shown by taking $\rho_p(t) = A\sin\omega t$, and $\rho(t) = (A+\varepsilon_1)\sin[(\omega+\varepsilon_2)t+\varepsilon_3]$, where $\varepsilon_{1\ldots3}$ are constant errors. Then it can be shown that

$$\lim_{t\to\infty}\delta = \left[A^2 + \frac{1}{2}\varepsilon_1^2 + A\varepsilon_1\right]^{1/2} \tag{51}$$

the term A^2 arises due to frequency and phase errors, whereas the rest of the terms arise due to amplitude errors. Therefore, as long as the function δ is observed to approach a constant value, the solution $\rho(t)$ is considered bounded. However, a secular drift from the nominal solution will lead to an increasing $\delta(t)$.

Numerical Simulations

Periodicity Condition

The efficacy of the initial condition result derived is demonstrated in this section. All simulations are performed by integrating the sixth-order ECI system of equations for each satellite. Furthermore, the periapsis for all examples is kept constant at $r_p = 7,100$ km, so that a can be obtained for any given e from the relation $a = r_p/(1-e)$. The purpose of this approach is to ensure that the satellite never approaches too near the surface of the Earth, for very high eccentricities.

First, the results derived will be used to set up a periodic relative orbit at an arbitrary epoch. For convenience, nondimensional units are chosen, although the simulations are based upon dimensional coordinates with time as the independent variable. The initial true anomaly, orbit size, and eccentricity are chosen as $f_i = 105$ deg, $e = 0.3$, and $\varrho_0 = 10$ km, respectively. The initial values of the states of the deputy satellite, denoted by $\boldsymbol{x}_i$, are chosen from the HCW initial conditions by setting $e = 0$, $\rho_1 = \rho_3 = 1$, $\rho_2 = 0$, and $\alpha = \beta = 30$ deg in Eq. (21). Therefore, $\mathbf{x}_{0_i} = \{0.5 \quad 1.732 \quad 0.5 \quad 0.866 \quad -10.866\}^T$ (nondimensional). Equation (20) can be used to obtain their values for a periodic orbit. Upon correction,

$$x'_{0_i} = 0.762, \quad y'_{0_i} = -1.331$$

By using the formulas derived, the correction required to negate secular drift induced by second-order differential gravity is found to be $y'_{1_i} = -2.386$. The trajectory with and without this correction is shown in Fig. 2. The broken line indicates the trajectory without the correction, and considerable drift can be seen after 5 orbits. The solid line indicates that the corrected trajectory effectively accounts for the second-order differential gravity terms and remains bounded.

To analyze the extent of efficiency of the correction developed, various cases are drawn from existing works in the literature. The following cases assume epoch at $f_i = 0$. First, comparisons are made with the eccentricity/nonlinearity correction from [20]. A reference orbit with $e = 0.05$ is chosen with $\varrho_0 = 10$ km. The initial conditions are chosen such that $\alpha = \beta = 0$ deg, $\rho_1 = 2\rho_3 = 1$, and $\rho_2 = 0$. Figure 3a shows the relative orbit using HCW initial conditions (without eccentricity and/or nonlinearity conditions), and using the correction developed in this paper. The broken line indicates the propagation using the HCW conditions for a period of 20 orbits, and it is evident that a large amount of drift is present. However, by using the corrected initial conditions, the orbit shows negligible deviation even after 20 orbits. Figure 3b shows the percentage drift calculated by using Eq. (50). It is observed that the uncorrected condition shows about 80% error, which is also directly observed from Fig. 3a. By using the correction for nonlinearity and eccentricity developed in [20], this error is reduced to 10% (correction 1). These errors agree with those from [20], for similar

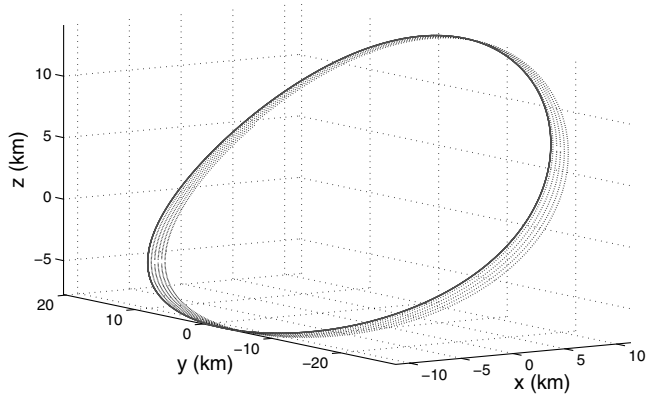

Fig. 2 Corrected and uncorrected relative orbit, $e = 0.3$, $f_i = 105$ deg.

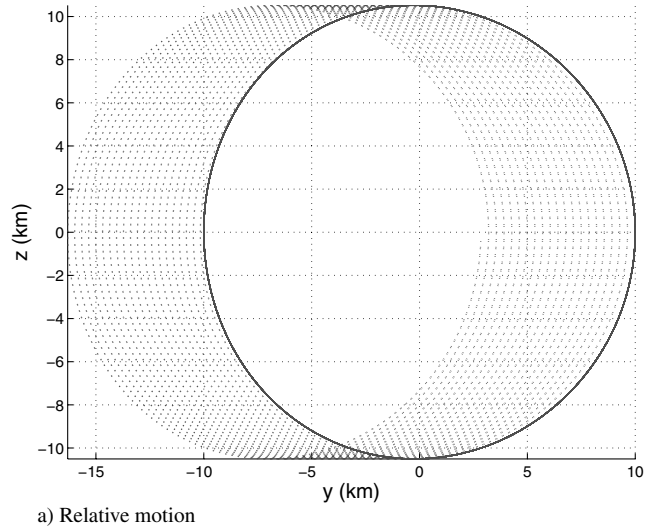

a) Relative motion

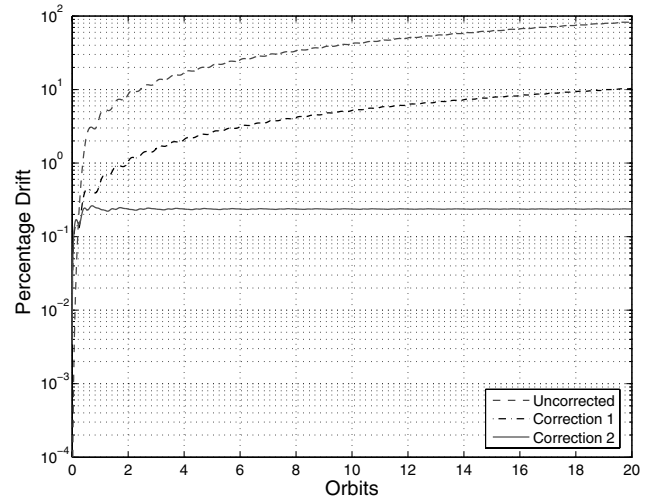

b) Drift from nominal solution

Fig. 3 Relative motion with corrected and uncorrected initial conditions $e = 0.05$, $f_i = 0$.

initial conditions. By using Eq. (40), this error is approximately 0.2% (correction 2).

Next, a comparison is made for a reference orbit with moderate eccentricity, where the result obtained by [20] fails, but where the zeroth-order eccentricity correction, also presented by [18], is expected to be valid. Figure 4a shows the relative orbit for $e = 0.2$ and $\varrho_0 = 10$ km. The deputy's orbit is initiated using the periodic equations in Eq. (21), setting $\rho_1 = 0.5$, $\rho_2 = 0.1$, $\rho_3 = 1.2$, and $\alpha = \beta = 0$ deg. It is evident that these initial conditions show secular

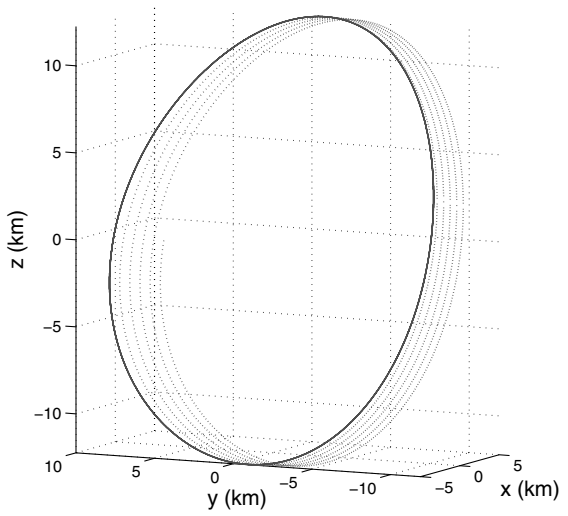

a) Relative motion

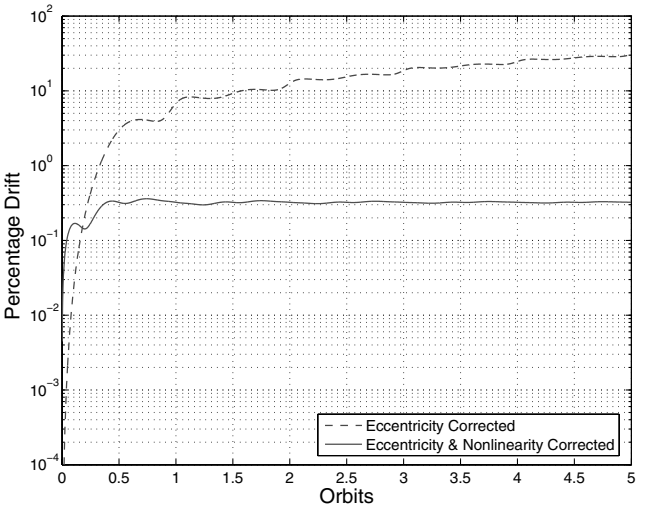

b) Drift from nominal solution

Fig. 4 Relative motion with corrected and uncorrected initial conditions $e = 0.2$, $f_i = 0$.

drift due to nonlinear differential gravity, as indicated by the broken line. However, by employing the correction derived, the drift is negligible even after five orbit periods, as indicated by the solid line. A study of the drift as shown in Fig. 4b shows that the nonlinearity correction results in an error of approximately 0.3% of the orbit size, as opposed to the linear condition, which shows approximately 12% drift and continues to increase.

Figure 5a shows an orbit with the chief's eccentricity selected as $e = 0.8$, all other values kept the same as in the previous case. In this case it is observed that the initial conditions that satisfy the linearized periodicity condition do not even lead to bounded motion, and the relative motion quickly diverges within one orbit period in the presence of nonlinear terms, as indicated by the broken line. The solid line shows that by using the correction developed in this paper, periodicity is maintained. As shown in Fig. 5b, the error after the correction is approximately 2% of the orbit size. Keeping in mind that the error functions for the corrected solution, as depicted in Figs. 3b, 4b, and 5b, approach constant values, these values only indicate the amplitude error as a result of the correction. The orbits themselves show negligible drift.

Accuracy of the Analytical Solution

The second-order analytical solution that has been developed in this paper is tested against numerical integration in a fully nonlinear

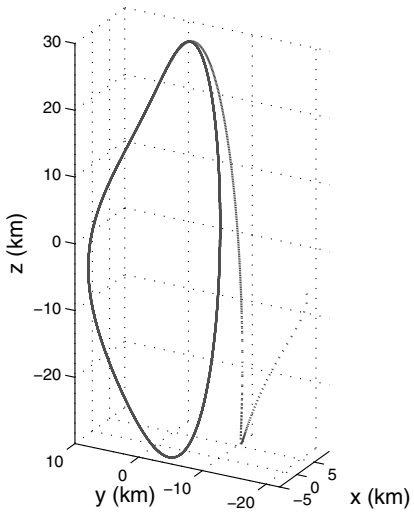

a) Relative motion

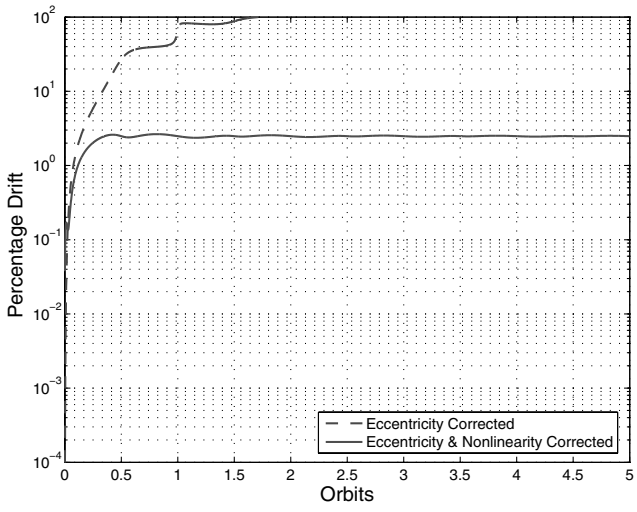

b) Drift from nominal solution

Fig. 5 Relative motion with corrected and uncorrected initial conditions $e = 0.8$, $f_i = 0$.

differential gravity environment. The reference orbit has $e = 0.4$ and $a = 12,000$ km. The relative orbit is of dimension $\varrho_0 = 20$ km, and the formation is initiated at $f_i = 30$ deg. The parameters for the relative orbit are: $\rho_1 = 0.4782$, $\rho_2 = 0.1729$, $\rho_3 = 0.9165$, $\alpha = -0.5236$, and $\beta = -0.5136$. The errors between integrated relative position and the relative position as predicted by the second-order analytical equations is shown in Fig. 6. It is observed that after five orbits, the error in position prediction is within 100 m. This is an error of less than 1%. Growth is observed in the error due to the contribution of terms of third and higher order.

Energy-Matching Criterion

The exact periodicity condition for formation flight is $\Delta a = 0$, or when the time periods of the chief and deputy are equal. However, the periodicity conditions based on the unperturbed TH equations and the perturbed TH equations, only approximately satisfy the equation $\Delta a = 0$. The extent to which this condition is satisfied can be measured if the initial conditions of the chief's and deputy's states in the local reference frame are converted to their respective inertial positions and velocities, and then to their respective orbital elements. A comparison of the uncorrected and nonlinear-corrected initial conditions is shown in Fig. 7. These results are for a reference orbit with $a = 40,000$ km, and $\varrho_0 = 10$ km, with epoch at $f_i = 0$. It is observed that even if the chief's eccentricity is 0.9, the difference between the deputy and chief semimajor axes is of the order of

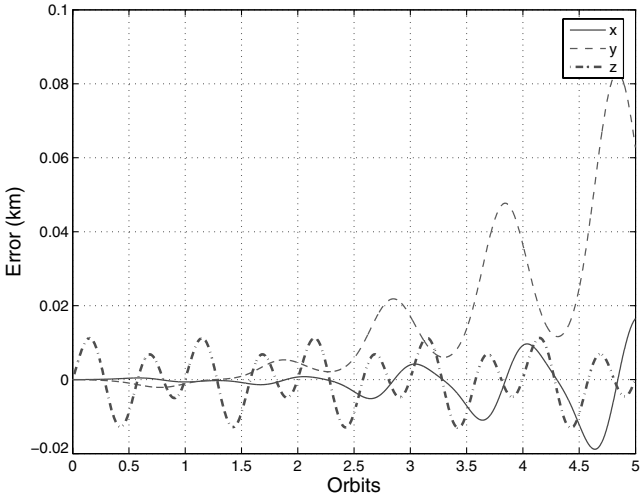

Fig. 6 Accuracy of the analytical solution.

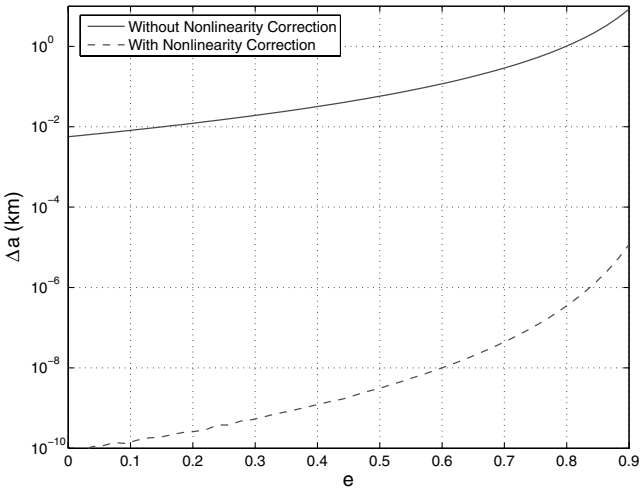

Fig. 7 Periodicity condition satisfaction using corrected and uncorrected initial conditions.

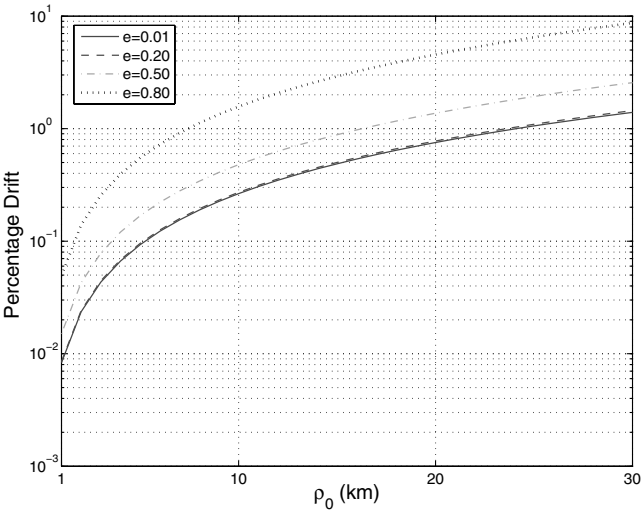

Fig. 8 Effect of nonlinearity and eccentricity on errors.

millimeters. Given the limitations of navigation technology, this is almost exact. In contrast, the uncorrected initial conditions lead to semimajor axis differences of hundreds of meters even for intermediate eccentricities, which lead to considerable drift in relative motion.

Effect of Eccentricity and Nonlinearity on Boundedness

It is now desired to study the efficacy of the correction under the effect of increasing ϱ_0. This is shown in Fig. 8. These simulations were carried out for 10 time periods of the reference, for a variety of eccentricity values, as indicated. The figure shows that for ϱ_0 up to 30 km, and even with moderate values of eccentricity, the error is less than 1%. However, for high eccentricities, such as those greater than 0.8, the error is shown to increase markedly. This is due to the fact that the combined effect of large ϱ_0 and large e leads to ϵ^2 and ϵ being of the same order, and thus third-order terms in Eq. (12) are no longer negligible in comparison with the second-order terms.

Conclusions

Phase space initial conditions for periodic relative motion have been developed for an orbit with arbitrary eccentricity, by treating second-order nonlinear differential gravity terms as perturbations to the Tschauner–Hempel equations. By identifying only those terms that contribute to secular growth in relative motion, a condition for ensuring periodic motion is easily obtained. These initial conditions are shown to work remarkably well under the most general conditions, including those with very high eccentricities, and can serve as excellent guesses for initiating a numerical procedure for matching the semimajor axes of the two satellites by correcting one of the relative motion initial conditions. The removal of secular growth terms leads to the formulation of analytical second-order relative motion equations that very accurately model relative orbits in terms of its parameters. These expressions can be used for stationkeeping algorithms and will require less fuel for relative orbit maintenance.

Appendix

Coefficients L_0, L_{c_k}, and L_{s_k}

$$L_0 = \frac{9e}{8}\rho_1^2\cos 2\alpha + 3\rho_1\rho_2\cos\alpha, \qquad L_{c_1} = -\frac{3}{8}\rho_3^2\cos 2\beta - \frac{3}{4}\rho_3^2 + \frac{3}{4}\rho_1^2\cos 2\alpha - \frac{3}{2}\rho_1^2 + \frac{3e^2}{16}\rho_1^2 + \frac{3e}{4}\rho_1\rho_2\cos\alpha - \frac{3}{2}\rho_2^2 + \frac{e^2}{4}\rho_1^2\cos 2\alpha$$

$$L_{s_1} = -\frac{e^2}{16}\rho_1^2\sin 2\alpha + \frac{3}{8}\rho_3^2\sin 2\beta - \frac{3}{4}\rho_1^2\sin 2\alpha + \frac{3e}{4}\rho_1\rho_2\sin\alpha, \qquad L_{c_2} = \frac{e}{4}\rho_1^2\cos 2\alpha, \qquad L_{s_2} = -\frac{e}{4}\rho_1^2\sin 2\alpha$$

$$L_{c_3} = \frac{e}{4}\rho_1\rho_2\cos\alpha + \frac{1}{8}\rho_3^2\cos 2\beta - \frac{1}{4}\rho_1^2\cos 2\alpha + \frac{e^2}{32}\rho_1^2\cos 2\alpha + \frac{e^2}{16}\rho_1^2, \qquad L_{s_3} = -\frac{e^2}{32}\rho_1^2\sin 2\alpha + \frac{1}{4}\rho_1^2\sin 2\alpha - \frac{e}{4}\rho_1\rho_2\sin\alpha - \frac{1}{8}\rho_3^2\sin 2\beta$$

$$L_{c_4} = -\frac{e}{8}\rho_1^2\cos 2\alpha, \qquad L_{s_4} = \frac{e}{8}\rho_1^2\sin 2\alpha, \qquad L_{c_5} = -\frac{e^2}{32}\rho_1^2\cos 2\alpha, \qquad L_{s_5} = \frac{e^2}{32}\rho_1^2\sin 2\alpha$$

Evaluating $\int L/\sin^2 f\,\mathrm{d}f$

$$\int \frac{1}{\sin^2 f}\,\mathrm{d}f = -\cot f, \qquad \int \frac{\sin f}{\sin^2 f}\,\mathrm{d}f = \ell_n\ \frac{(1-\cos f)}{\sin f}, \qquad \int \frac{\cos f}{\sin^2 f}\,\mathrm{d}f = -\mathrm{cosec} f, \qquad \int \frac{\sin 2f}{\sin^2 f}\,\mathrm{d}f = 2\ \ell_n\ \sin f$$

$$\int \frac{\cos 2f}{\sin^2 f}\,\mathrm{d}f = -\cot f - 2f, \qquad \int \frac{\sin 3f}{\sin^2 f}\,\mathrm{d}f = 4\cos f + 3\ \ell_n\ \frac{(1-\cos f)}{\sin f}, \qquad \int \frac{\cos 3f}{\sin^2 f}\,\mathrm{d}f = -3\mathrm{cosec} f + 2\frac{\cos 2f}{\sin f}$$

$$\int \frac{\sin 4f}{\sin^2 f}\,\mathrm{d}f = 2\cos 2f + 2 + 4\ \ell_n\ \sin f, \qquad \int \frac{\cos 4f}{\sin^2 f}\,\mathrm{d}f = -2\cot f + \frac{\cos 3f}{\sin f} - 4f$$

$$\int \frac{\sin 5f}{\sin^2 f}\,\mathrm{d}f = \frac{4}{3}\cos 3f + 8\cos f + 5\ \ell_n\ \frac{(1-\cos f)}{\sin f}, \qquad \int \frac{\cos 5f}{\sin^2 f}\,\mathrm{d}f = -5\mathrm{cosec} f + \frac{2}{3}\frac{\cos 4f}{\sin f} + \frac{10}{3}\frac{\cos 2f}{\sin f}$$

Evaluating $\int L/\phi^2 df$

$$\int \frac{1}{\phi^2}\,\mathrm{d}f = 2eH(f) - \frac{1}{\phi^2}\frac{\sin 2f}{2}, \qquad \int \frac{\cos f}{\phi^2}\,\mathrm{d}f = -\frac{2}{3}(2+e^2)H(f) + \frac{1}{\phi^2}\left[\frac{e}{6}\sin 2f - \frac{1}{3}\sin 3f - \frac{e}{12}\sin 4f\right]$$

$$\int \frac{\cos 2f}{\phi^2}\,\mathrm{d}f = \frac{2}{3e}(2+e^2)H(f) + \frac{1}{\phi^2}\left[-\frac{1}{e}\sin f - \frac{2}{3}\sin 2f + \frac{1}{3e}\sin 3f + \frac{1}{12}\sin 4f\right]$$

$$\int \frac{\cos 3f}{\phi^2}df = -2(2-e^2)H(f) + \frac{1}{\phi^2}\left[-\sin f - \frac{e}{2}\sin 2f + \frac{e}{4}\sin 4f\right]$$

$$\int \frac{\cos 4f}{\phi^2}\,\mathrm{d}f = -\frac{2}{3e^3}(8 - 24e^2 + 13e^4)H(f) - \frac{8}{e^2}f + \frac{1}{\phi^2}\left[\frac{4}{e^3}(1+e^2)\sin f + \frac{1}{6e^2}(4+13e^2)\sin 2f\right.$$
$$\left. - \frac{4}{3e^3}(1+e^2)\sin 3f - \frac{1}{3e^2}(1+4e^2)\sin 4f\right]$$

$$\int \frac{\cos 5f}{\phi^2}\,\mathrm{d}f = -\frac{2}{3e^4}(-32 + 80e^2 - 50e^4 + 5e^6)H(f) + \frac{32}{e^3}f + \frac{1}{\phi^2}\left[-\frac{1}{e^4}(16 + 24e^2 + e^4)\sin f - \frac{1}{6e^3}(16 + 96e^2 - 5e^4)\sin 2f\right.$$
$$\left. + \frac{1}{3e^4}(16 + 24e^2 - 5e^4)\sin 3f + \frac{1}{12e^3}(16 + 96e^2 - 5e^4)\sin 4f + \sin 5f\right]$$

$$(1-e^2)^2\int\frac{\sin f}{\phi^2}\,\mathrm{d}f=\frac{1}{2}(1-e)^2\,\ell_n(1-\cos f)-\frac{1}{2}(1+e)^2\,\ell_n(1+\cos f)+2e\;\ell_n\;(1+e\cos f)-\frac{e(1-e^2)}{1+e\cos f}$$

$$(1-e^2)^2\int\frac{\sin 2f}{\phi^2}\,\mathrm{d}f=(1-e)^2\,\ell_n(1-\cos f)+(1+e)^2\,\ell_n(1+\cos f)-2(1+e^2)\,\ell_n(1+e\cos f)+\frac{2(1-e^2)}{1+e\cos f}$$

$$(1-e^2)^2\int\frac{\sin 3f}{\phi^2}\,\mathrm{d}f=\frac{3}{2}(1-e)^2\,\ell_n(1-\cos f)-\frac{3}{2}(1+e)^2\,\ell_n(1+\cos f)+6e\;\ell_n(1+e\cos f)-\frac{(4-e^2)}{e}\frac{(1-e^2)}{1+e\cos f}$$

$$(1-e^2)^2\int\frac{\sin 4f}{\phi^2}\,\mathrm{d}f=2(1-e)^2\,\ell_n(1-\cos f)+2(1+e)^2\,\ell_n(1+\cos f)+\frac{4}{e^2}(2-5e^2+e^4)\,\ell_n(1+e\cos f)+\frac{4(2-e^2)}{e^2}\frac{(1-e^2)}{1+e\cos f}$$

$$(1-e^2)^2\int\frac{\sin 5f}{\phi^2}\,\mathrm{d}f=\frac{5}{2}(1-e)^2\,\ell_n(1-\cos f)-\frac{5}{2}(1+e)^2\,\ell_n(1+\cos f)+\frac{16}{e^2}(1-e^2)^2\cos f-\frac{2}{e^3}(16-32e^2+11e^4)\,\ell_n(1+e\cos f)$$
$$-\frac{(16-12e^2+e^4)}{e^3}\frac{(1-e^2)}{1+e\cos f}$$

Coefficients C_k, D_k, E_k, F_k, G_k, and H_k

$$C_1=\frac{e}{4}\rho_1^2\cos 2\alpha+2\rho_1\rho_2\cos\alpha+\frac{e}{2}\rho_1^2-\frac{1}{e}(2\rho_1^2+2\rho_2^2+\rho_3^2),\qquad C_2=\frac{1}{2}\rho_1^2\cos 2\alpha-\frac{1}{4}\rho_3^2\cos 2\beta-\frac{1}{4}(2\rho_1^2+2\rho_2^2+\rho_3^2)$$

$$C_3=\frac{e}{12}\rho_1^2\cos 2\alpha,\qquad D_0=\rho_1^2\left(\frac{1}{4}-\frac{1}{2e^2}\right)\sin 2\alpha+\frac{1}{2e^2}\rho_3^2\sin 2\beta+\frac{1}{e}\rho_1\rho_2\sin\alpha,\qquad D_1=\rho_1^2\left(\frac{e}{4}-\frac{1}{e}\right)\sin 2\alpha+\frac{1}{e}\rho_3^2\sin 2\beta+2\rho_1\rho_2\sin\alpha$$

$$D_2=\frac{1}{4}\rho_1^2\sin 2\alpha,\qquad D_3=\frac{e}{12}\rho_1^2\sin 2\alpha,\qquad E_1=-\frac{3e}{4}\rho_1^2\cos 2\alpha-3\rho_1\rho_2\cos\alpha,\qquad F_1=-\frac{3e}{4}\rho_1^2\sin 2\alpha-3\rho_1\rho_2\sin\alpha$$

$$E_2=-\frac{3}{4}\rho_1^2\cos 2\alpha,\qquad F_2=-\frac{3}{4}\rho_1^2\sin 2\alpha,\qquad E_3=-\frac{e}{12}\rho_1^2\cos 2\alpha,\qquad F_3=-\frac{e}{12}\rho_1^2\sin 2\alpha,\qquad G_1=D_1/2,\qquad G_2=D_2$$

$$G_3=3D_3/2,\qquad H_0=-\frac{e^2}{16}\rho_1^2\cos 2\alpha-\frac{e}{2}\rho_1\rho_2\cos\alpha+\left(\frac{1}{2}-\frac{e^2}{8}\right)\rho_1^2+\frac{1}{2}\rho_2^2+\frac{1}{4}\rho_3^2$$

$$H_1=-\frac{7e}{8}\rho_1^2\cos 2\alpha-3\rho_1\rho_2\cos\alpha-\frac{e}{8}\rho_3^2\cos 2\beta-\frac{e}{8}(2\rho_1^2+2\rho_2^2+\rho_3^2)$$

$$H_2=-\frac{1}{8}(4+e^2)\rho_1^2\cos 2\alpha-\frac{e}{2}\rho_1\rho_2\cos\alpha+\frac{1}{4}\rho_3^2\cos 2\beta+\left(1-\frac{e^2}{8}\right)\rho_1^2+\rho_2^2+\frac{1}{2}\rho_3^2$$

$$H_3=-\frac{3e}{8}\rho_1^2\cos 2\alpha+\frac{e}{8}\rho_3^2\cos 2\beta+\frac{e}{8}(2\rho_1^2+2\rho_2^2+\rho_3^2),\qquad H_4=-\frac{e^2}{16}\rho_1^2\cos 2\alpha$$

Acknowledgments

The authors wish to thank Kyle T. Alfriend for his help through insightful discussions.

References

[1] Carpenter, J. R., Leitner, J. A., Folta, D. C., and Burns, R. D., "Benchmark Problems for Spacecraft Formation Flight Missions," *AIAA Guidance, Navigation, and Control Conference and Exhibit*, AIAA Paper 2003-5364, Aug. 2003.

[2] Curtis, S. A., "The Magnetosphere Multiscale Mission...Resolving Fundamental Processes in Space Plasmas," NASA, TM-2000-209883, 1999.

[3] Clohessy, W. H., and Wiltshire, R. S., "Terminal Guidance System for Satellite Rendezvous," *Journal of Aerospace Sciences*, Vol. 27, Sept. 1960, pp. 653–658, 674.

[4] Knollman, G. C., and Pyron, B. O., "Relative Trajectories of Objects Ejected from a Near Satellite," *AIAA Journal*, Vol. 1, No. 2, 1963, pp. 424–429.

[5] London, H. S., "Second Approximation to the Solution of Rendezvous Equations," *AIAA Journal*, Vol. 1, No. 7, 1963, pp. 1691–1693.

[6] Karlgaard, C. D., and Lutze, F. H., "Second-Order Relative Motion Equations," *Journal of Guidance, Control, and Dynamics*, Vol. 26, No. 1, 2003, pp. 41–49.

[7] Richardson, D. L., and Mitchell, J. W., "A Third-Order Analytical Solution for Relative Motion with a Circular Reference Orbit," *Journal of the Astronautical Sciences*, Vol. 51, No. 1, 2003pp. 1–12.

[8] Tschauner, J., and Hempel, P., "Rendezvous zu Einemin Elliptischer Bahn Umlaufenden Ziel," *Acta Astronautica*, Vol. 11, No. 2, 1965, pp. 104–109.

[9] De Vries, J. P., "Elliptic Elements in Terms of Small Increments of Position and Velocity Components," *AIAA Journal*, Vol. 1, No. 11, 1963, pp. 2626–2629.

[10] Kolemen, E., and Kasdin, N. J., "Relative Spacecraft Motion: A Hamiltonian Approach to Eccentricity Perturbations," *AAS/AIAA Spacecraft Mechanics Meeting*, Vol. 119, Advances in the Astronautical Sciences, Univelt, Escondido, CA, 2004, pp. 3075–3086; also American Astronautical Society Paper 04-294.

[11] Lawden, D. F., *Optimal Trajectories for Space Navigation*, Butterworths, London, 1967, pp. 79–95.

[12] Carter, T. E., and Humi, M., "Fuel-Optimal Rendezvous Near a Point in General Keplerian Orbit," *Journal of Guidance, Control, and Dynamics*, Vol. 10, No. 6, 1987, pp. 567–573.

[13] Carter, T. E., "New Form for the Optimal Rendezvous Equations Near a Keplerian Orbit," *Journal of Guidance, Control, and Dynamics*, Vol. 13, No. 1, 1990, pp. 183–186.

[14] Wolfsberger, W., Weiß, J., and Rangnitt, D., "Strategies and Schemes for Rendezvous on Geostationary Transfer Orbit," *Acta Astronautica*, Vol. 10, No. 8, 1983, pp. 527–538.

[15] Yamanaka, K., and Ankersen, F., "New State Transition Matrix for Relative Motion on an Arbitrary Elliptical Orbit," *Journal of Guidance, Control, and Dynamics*, Vol. 25, No. 1, 2002, pp. 60–66.

[16] Melton, R. G., "Time Explicit Representation of Relative Motion Between Elliptical Orbits," *Journal of Guidance, Control, and Dynamics*, Vol. 23, No. 4, 2000, pp. 604–610.

[17] Broucke, R. A., "Solution of the Elliptic Rendezvous Problem with the Time as Independent Variable," *Journal of Guidance, Control, and Dynamics*, Vol. 26, No. 4, 2003, pp. 615–621.

[18] Inalhan, G., Tillerson, M., and How, J. P., "Relative Dynamics and Control of Spacecraft Formations in Eccentric Orbits," *Journal of Guidance, Control, and Dynamics*, Vol. 25, No. 1, 2002, pp. 48–59.

[19] Anthony, M. L., and Sasaki, F. T., "Rendezvous Problem for Nearly Circular Orbits," *AIAA Journal*, Vol. 3, No. 9, 1965, pp. 1666–1673.

[20] Vaddi, S. S., Vadali, S. R., and Alfriend, K. T., "Formation Flying:

Accommodating Nonlinearity and Eccentricity Perturbations," *Journal of Guidance, Control, and Dynamics*, Vol. 26, No. 2, 2003, pp. 214–223.

[21] Gurfil, P., "Relative Motion Between Elliptic Orbits: Generalized Boundedness Conditions and Optimal Formationkeeping," *Journal of Guidance, Control, and Dynamics*, Vol. 28, No. 4, 2005, pp. 761–767.

[22] Euler, E. A., and Shulman, Y., "Second-Order Solution to the Elliptic Rendezvous Problem," *AIAA Journal*, Vol. 5, No. 5, 1967, pp. 1033–1035.

[23] Alfriend, K. T., Schaub, H., and Gim, D.-W., "Gravitational Perturbations, Nonlinearity and Circular Orbit Assumption Effects on Formation Flying Control Strategies," *AAS Guidance and Control Conference*, Vol. 104, Advances in the Astronautical Sciences, Univelt, Escondido, CA, 2000, pp. 139–158; also American Astronautical Society Paper 00-012.

[24] Vadali, S. R., Vaddi, S. S., and Alfriend, K. T., "A New Concept for Controlling Formation Flying Satellite Constellations," *AAS/AIAA Spaceflight Mechanics Meeting*, Vol. 108, Advances in the Astronautical Sciences, Univelt, Escondido, CA, 2001, pp. 1631–1648; also American Astronautical Society Paper 01-218.

[25] Schaub, H., "Relative Orbit Geometry Through Classical Orbit Element Differences," *Journal of Guidance, Control, and Dynamics*, Vol. 27, No. 5, 2004, pp. 839–848.

[26] Garrison, J. L., Gardner, T. G., and Axelrad, P., "Relative Motion in Highly Elliptical Orbits," *AAS/AIAA Spaceflight Mechanics Meeting*, Vol. 89, Advances in the Astronautical Sciences, Univelt, Escondido, CA, 1995, pp. 1359–1376; also American Astronautical Society Paper 95-194.

[27] Sabol, C., McLaughlin, C. A., and Luu, K. K., "Meet the Cluster Orbits with Perturbations of Keplerian Elements (COWPOKE) Equations," *AAS/AIAA Spaceflight Mechanics Meeting*, Vol. 114(3), Advances in the Astronautical Sciences, Univelt, Escondido, CA, 2003, pp. 573–594; also American Astronautical Society Paper 03-138.

[28] Sengupta, P., Vadali, S. R., and Alfriend, K. T., "Modeling and Control of Satellite Formations in High Eccentricity Orbits," *Journal of the Astronautical Sciences*, Vol. 52, No. 1–2, 2004, pp. 149–168.

[29] Battin, R. H., *An Introduction to the Mathematics and Methods of Astrodynamics*, revised ed., AIAA, Reston, VA, 1999, pp. 110–116, 158–164.

[30] Alfriend, K. T., Yan, H., and Vadali, S. R., "Nonlinear Considerations in Satellite Formation Flying" *AIAA/AAS Astrodynamics Specialist Conference*, Paper 2002-4741, Aug. 2002.

[31] Kechichian, J. A., "Motion in General Elliptic Orbit with Respect to a Dragging and Precessing Coordinate Frame," *Journal of the Astronautical Sciences*, Vol. 46, No. 1, 1998, pp. 25–46.

[32] Nayfeh, A. H., *Perturbation Methods*, Wiley, Hoboken, NJ, 1973, pp. 23–55.

[33] Sengupta, P., and Vadali, S. R., "Formation Design and Geometry for Keplerian Elliptic Orbits with Arbitrary Eccentricity," American Astronautical Society Paper 06-161, Jan. 2006.